Materials and Manufacturing Processes

ISSN: (Print) (Online) Journal homepage: https://www.tandfonline.com/loi/lmmp20

Manufacture of bone fracture plates based on glass fiber reinforced polyurethane composite: a gravity casting adapted process

Flaminio C. P. Sales, P. Ana de Moura, Romeu R. C. da Costa & João E. Ribeiro

To cite this article: Flaminio C. P. Sales, P. Ana de Moura, Romeu R. C. da Costa & João E. Ribeiro (2022): Manufacture of bone fracture plates based on glass fiber reinforced polyurethane composite: a gravity casting adapted process, Materials and Manufacturing Processes, DOI: 10.1080/10426914.2022.2072876

To link to this article: https://doi.org/10.1080/10426914.2022.2072876

MATERIALS AND MANUFACTURING PROCESSES
https://doi.org/10.1080/10426914.2022.2072876

Taylor & Francis
Taylor & Francis Group

Manufacture of bone fracture plates based on glass fiber reinforced polyurethane composite: a gravity casting adapted process

Flaminio C. P. Sales[a,b], P. Ana de Moura[b], Romeu R. C. da Costa[b], and João E. Ribeiro[a,c]

[a]Instituto Politécnico de Bragança, Bragança, Portugal; [b]Department of Mechanical Engineering, Federal University of Technology - Paraná (UTFPR), Cornélio Procópio, Brazil; [c]Mountain Research Center, Instituto Politécnico de Bragança, Bragança, Portugal

ABSTRACT

The development of materials and devices to replace or restore damaged tissue functions has a prominent position in the scientific community, promoting the interest for metal-free alternatives, like composites. These proved to be a promising option as, besides new matrix and reinforcement combinations, new manufacturing methods tend to fulfil tailored requirements of the medical field. In this sense, we manufactured glass fiber/polyurethane composite plates for Osteosynthesis. Models based on commercial LCP implants were 3D printed and used to generated molds through a new adapted resin casting process. Additional mechanical tests showed that reinforcement additions between 10 wt% and 25 wt% caused an increase in the bending structural stiffness by 126%-165% when compared to pure polymer implants. In addition, if the number of holes is increased, from 4 to 6, the maximum stress reduces by 40%. The manufacturing process was an effective alternative as it presented low cost, high customization and allowed the development of complex geometries, resin injection and degassing.

ARTICLE HISTORY
Received 31 August 2021
Accepted 31 March 2022

KEYWORDS
Plates for osteosynthesis; manufacturing process; fracture healing; gravity casting; biomaterials

1. Introduction

The human quality of life has been changing due to the constant technological advances, resulting on an increased life expectancy of the world population.[1–3] Therefore, age-related diseases rates also raised, including the ones associated with bone structure, such as osteoporosis, osteoarthrosis and loss of bone mass.[4,5] Furthermore, the occurrence of bone tissue trauma caused by accidents[6] and the lack of care or hygiene (for example, tooth loss) can also affect young individuals in their more productive phase, causing a relevant socioeconomic impact.[7–9]

Over the past century, materials and devices have been developed to successfully replace or restore the functions of diseased or damaged tissues.[10] Metals have been chosen since the 60's as the main material used in the manufacture of implants such as fracture plates.[11] However, metallic devices can cause stress shielding, a phenomenon caused by the much higher strength and stiffness of the material when compared with bones. In addition, its cost is considered high in many countries that reusing of old plates has already been studied as an economic alternative. For instance, researches carried out in 2002, from the United States Food and Drug Administration (FDA), showed that reusing single-use devices could lead to cost savings, to the patient, of approximately 30%.[12,13] Thus, alternative materials that present mechanical properties closer to the human bone and are biocompatible have been researched.[14–17]

Composites are a great alternative as they have wide tailored characteristics, obtained from the combination of two or more materials taking advantage of desired features from each one.[18] Thereby, the development of fiber-reinforced composites (FRC) has created a new perspective in the metal-free medical field and led the development of new production methods; with improvements in aesthetic mechanical, biological and adhesive properties.[19,20]

Among synthetic reinforcements, glass fibers are the most widespread option, as it is an amorphous material with easy and low-cost processing.[21,22]

Concerning the matrix, some polymeric options as polyurethane (PU) are biocompatible, nontoxic, have excellent structural properties, good adhesion power, and are low cost.[23,24] PU is a thermoset polymer that has large applications in the health field, especially in orthopedics as bone substitute and it is fully compatible with living organisms, with no rejection. Still, biocalcification and osteointegration of polyurethane prothesis were reported.[25,26] Despite the advantages of these materials using, few studies have reported about composite bone plate manufacturing.[27]

To carry out the composites manufacturing, there are several processes. However, part of them are not applicable for unidirectional fibers or are slow and not able to reproduce complex geometries.[28,29]

Most of the authors who studied composite bone plates used hot processing with metallic molds, such as heat-compressing, more suitable for thermoplastic or for semi-cured thermoset molding compounds.[30] Examples are the researches done by: Fujiahara et al (2001), with braid carbon/PEEK (Polyetheretherketone)[31]; by Kabiri et al (2020), who worked with glass fibers/polypropylene[32]; and by PARK et al 2012, that also used a glass/PP (polypropylene) composite.[33] However, this technique is considered complex because the pressure, temperature and curing time

CONTACT João E. Ribeiro jribeiro@ipb.pt ESTiG, Instituto Politécnico de Bragança, Bragança 5300-052, Portugal

This article has been corrected with minor changes. These changes do not impact the academic content of the article.

should be precisely applied for each composite material. If the pressure used is extremely high fibers breakage can occur; on the other hand, pressure lower than an ideal value (defined for each material) may generate poor interface adhesion. High temperatures can change the material final properties and cause poor mechanical results, still, if the temperature is below the requirement, the fiber will not be impregnated due to the higher viscosity of the matrix, since in polymers when the working temperature reduces, usually, the viscosity increases.[34,35]

Arumugam et al (2020), made a plane prosthesis of epoxy reinforced with hybrid glass fibers/sisal using the hand layup technique. Their implants were cut from a plane sheet and did not have the under-surface contours, which are recommended to this application.[36] Also, the process was only suitable for stacking fabrics and did not allow changes or high control of the composite thickness.[28]

Hence, this work manufactured plates for Osteosynthesis (bone plates), based on PU reinforced with unidirectional E-type roving glass fibers (E-glass). The new manufacturing process was a resin casting adaptation that presented high flexibility as it was suitable for thermoset polymeric matrix and allowed changes before and during the manufacturing, due to quick model's changes based on 3D parameterized geometries, fiber amount increase and the drilling of holes according to each clinical scenario. Additionally, the process was low-cost and simple, because the adapted gravity casting does not need high-pressure inputs, metallic molds or heating systems. Lastly, it was able to replicate complex geometries using 3D printing to create silicone molds.

Along with that, four-point bending tests were conducted to evaluate if the mechanical properties, such as the stiffness, were similar to those presented by the bones, which would avoiding stress shielding and validate the process.

2. Materials and methods

2.1. Geometry and master pattern generation

The Locking Compressive Plates (LCP) geometry was chosen as it is considered one of the most advanced models of plates for Osteosynthesis, due to its recent development and great treatment flexibility, whenever opted by the surgeon.[37] After 1995, researches about this model increased and has been a clinical success, drawing the attention of a large number of manufacturers.[38]

The relation for the length of LCP plates in respect to the number of holes (n), the distance between holes (A), and the distance from the outermost hole to the end of the plate was taken through observations of commercial catalogs, osteosynthesis and fracture manuals.[39] This relation can be expressed by:

$$L = (n - 1) * A + 2 * B \quad (1)$$

For a 4.5 mm thick and 12.5 mm wide plate, A is equal to 18 mm, and B is 13 mm.

These relations were used to generate 3D Models for an external part (envelope) using SolidWorks® 2019 software, to speed up any future modifications.

The model designed could bear up to 6 screws. Likewise, implants without holes were produced, giving another degree of freedom for the surgeon: rather than opt for a cortical or locking screw hole, with pre-defined positions, when using a composite implant, it is possible to drill holes in the position desired, that enables better fracture stabilization, according to each clinical case.

Additionally, an inner part (core), was modeled, in which, the fibers were pre-impregnated before being taken to the final mold. Figure 1 represent the 3D models for LCP, modified straight LCP plates and this inner part.

2.2. Mold manufacturing

Using a gravity casting process, showed on Fig. 2, two bipartite molds were created for the core region and the final plates. The first 2-part mold, for internal regions can create up to 3 parts at each molding process and have ducts to resin admittance and air outlet. In these channels, a piston was used to inject the polymer and a vacuum pump was coupled to help on the liquid flow and degas process. Moreover, positioners were made to avoid any movement between the mold sides.

Regions were created inside the mold to hold the fiber and lock the roving ends, ensuring right alignment of the fiber Besides that, spacers were generated to facilitate the alignment of the core inside the final plate mold.

The second mold, for final plates, was simpler, it could create only one plate per casting and had assembled pieces to create the inlet and outlet ducts.

Silicone rubber was selected to manufacture the molds, being one material broadly used due to its capability to replicate complex geometries and achieve nanometer surface finishing. Furthermore, to produce the master pattern, 3D printing methods were used as they can ensure fine resolution, reaching micrometer scales.[40]

All master patterns were 3D printed with PLA 0.06 mm resolution by fused deposition modeling (FDM) using a Ultimaker©3 machine. After that, the printed pieces were positioned inside a delimited box before the elastomer pour.

The elastomer used (AE SA 13 INC) was an addition silicone, bicomponent, with a mixing ratio equal to 1:1 (base to curing agent), distributed by "Atelier do Escultor". It was degassed on a vacuum chamber before the stirring process, which was done manually until it reached complete homogeneity. Following that, a second degas was done for 10 minutes.

Subsequently, the liquid was poured into the delimited box and the curing process was performed for 4 hours at room temperature.

Then, the master pattern was removed. For the final plate matrix, it was necessary to disassemble the pieces and create a little incision to remove it.

2.3. Material resin casting

The material resin casting technique was adapted and divided into two steps. First, an inner part, with oriented fiber, was made. After, the inner piece was positioned inside of another mold to complete the implants' geometry by adding more polyurethane.

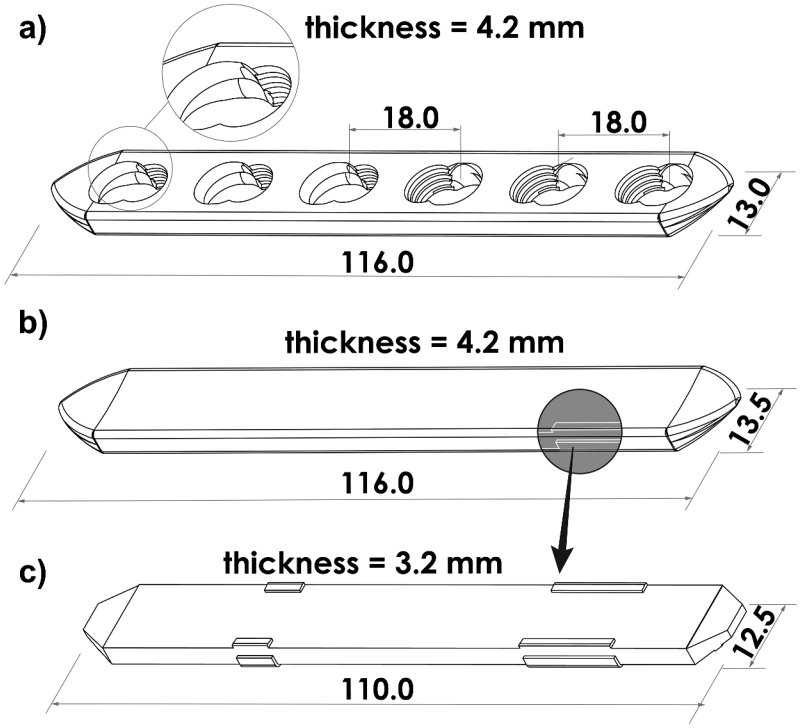

Figure 1. 3D models for 4.5mm 6 holes plates: (a) Original LCP based on commercial dimensions. (b) Modified LCP without holes with a section showing the internal part (c) Inner core.

Firstly, the unidirectional, E-type, roving glass fibers (E-glass) or the inner part was inserted and positioned inside the mold and closed. Six, nine or fourteen roving portions were positioned. Any of these pieces had 0.18 grams, resulting in final plates with 10–11.5 grams. Due to the variation of the number of roving portions in each sample, the fiber mass fractions in the final plates were around 10, 15 and 25 wt%, respectively.

The polyurethane was the SikaForce 7710L100 bicomponent, mixed in a 100:19 mass ratio. After mixing, a degas was carried out, then the resin was heated at 50°C for 5 minutes to reduce its viscosity.

The matrix was poured into the inlet duct and a vacuum pump was connected into the outlet channel. Intermittent vacuum degassing reduced the bubbles generated by the pouring. The curing process took 2 hours and 30 minutes inside a 50°C heating chamber.

Since the generated implants had enough size to 6 screw positioning at maximum, two groups were drilled with a 4.5 mm diameter drill bit: one with 6 holes and another with 4 spaces for screw insertions near the crack gap and on the distal fracture positions. Some of the samples made by the presented methodology are shown in Fig. 3.

2.4. Bending test

The 4-points bending properties for the 6 samples sets were evaluated in a Shimadzu® Autograph AGS-X 10KN universal testing machine. Each group had at least 5 specimens with the fiber mass fraction and hole number as presented in Table 1. An average fiber fraction (15 wt%) was selected to evaluate the holes drilling effect on the final mechanical response and samples were named according to the amount of fiber used (0%F, 10%GF, 15%F and 25%F) and the number of drilled holes (0 H, 4 H or 6 H). For instance, 15%F6 H means this sample has 15%wt of glass fiber and 6 holes.

All the test procedures were based on ISO 9585 standards.[41] The distance between upper load rollers (k) was 36 mm and the space between an upper roller and the nearest support roller (h) was 18 mm, as shown in Fig. 4. Constant displacement of 1 mm/min downward and a 1N pre-load were applied.

Using the data collected for load and displacement, the bending moment (M), in Nm, was calculated as the moment necessary to produce an offset displacement of 0.2% in the plate and is presented in Eq. 2. "P" represents the load reached at the proof point.

$$M = (Ph)/2[Nm] \tag{2}$$

After determining the slope of the initial point of the curve load versus displacement (S), also referred to as bending stiffness, the bending structural stiffness (EIe) was obtained by:

$$EIe = (2h + 3k)Sh/12\left[Nm^2\right] \tag{3}$$

Even though the material's behavior is orthotropic, equations from the beam theory can be used in a practical way to calculate the maximum stress on the outer surface. This approach has already been used with fiber reinforced composite in some works.[33,42] Maximum stress, which represents the flexural strength, was calculated according to the beam theory,[43] whereas "c" is the distance from the most outer fiber to the neutral axis, equal to 2.23 mm for the studied geometry and moment of inertia or second-order moment (I) was 81.92 mm^4. Both values were obtained using SolidWorks' properties section.

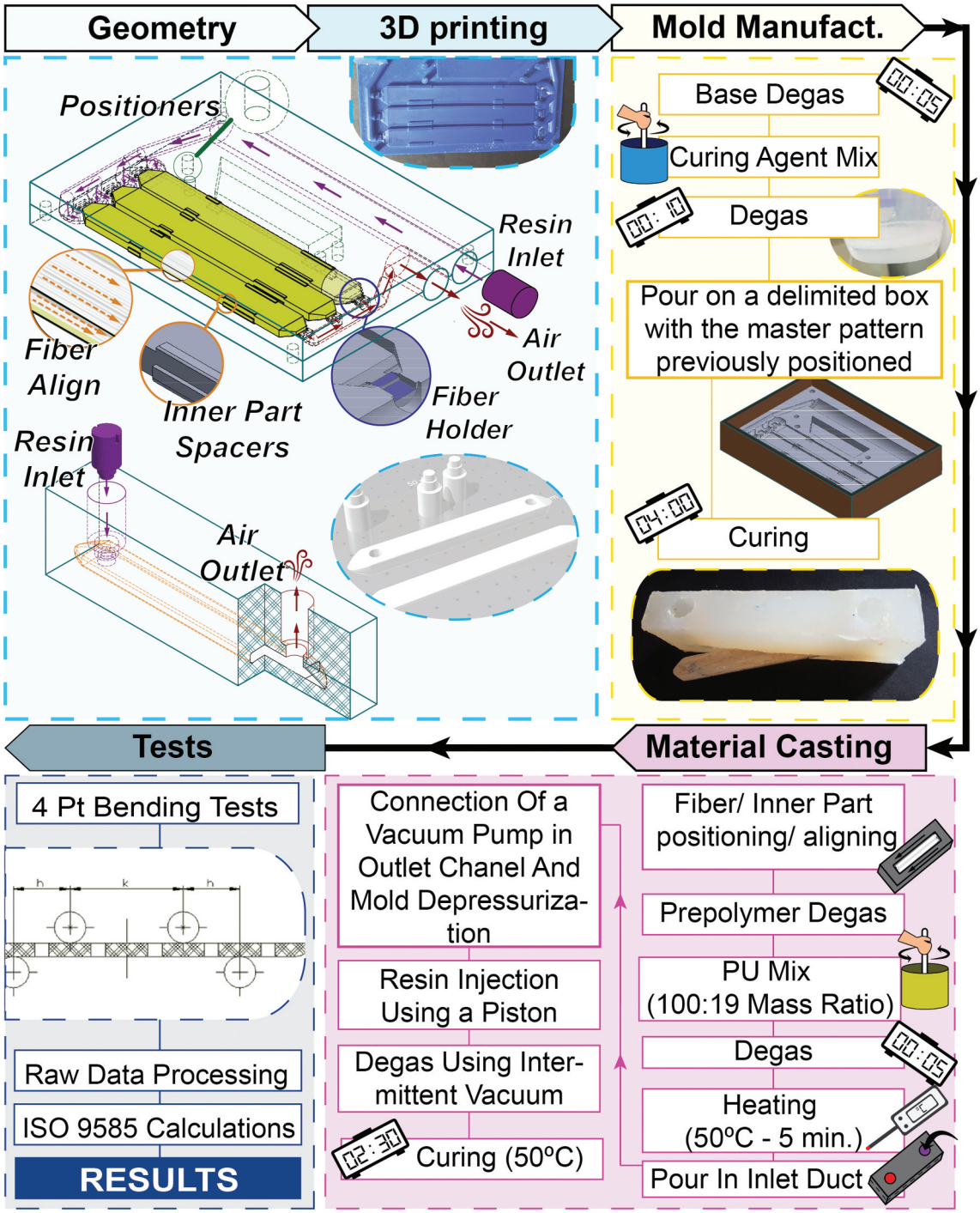

Figure 2. All the steps of the manufacturing process and bending tests.

$$\sigma_{max} = Mc/I[Pa] \quad (4)$$

2.5. Scanning electron microscopy

After the bending tests, samples were frozen at −18ºC for 12 h and broken manually to expose regions rich in fibers. In addition, the remaining faces of the samples were also cut until surface areas of around 5 mm^2 were reached, the necessary size for placement in the microscopy equipment.

The images were taken using a Phenom Pro Desktop scanning electron microscope from Thermo Fisher Scientific (Eindhoven, The Netherlands), which covered a sample region of approximately 1.25 mm^2 by using a zoom in a magnitude of 215 times This magnitude value

Figure 3. Composite plates made by an adapted resin casting method.

Table 1. Composition of composite plates tested in 4-point bending.

	0%wt E-glass	10%wt E-glass	15%wt E-glass	25%wt E-glass
0 Holes	0%F0 H	10%F0 H	15%F0 H	25%F0 H
4 Holes	-	-	15%F4 H	-
6 Holes	-	-	15%F6 H	-

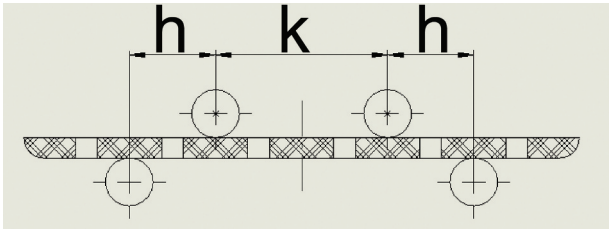

Figure 4. Support rollers and load rollers setup, whereas, h is equal to 18mm, and k is equal to 36mm.

was used later together with the sample area captured in the electron microscope, in order to generate scales, which allowed correct measurement of the fibers and pores. The equipment was managed by its own software (Phenon ProSuite) and images of the morphology, pores and fiber distribution in the samples were obtained.

3. Results

Load versus displacement curves were plotted for each sample as Fig. 5a shows. The graph represents the mean calculation of the results obtained from each sample tested. Also, standard deviations were calculated and are showed in the same image. Besides that, the behavior of a 15%F4 H specimen at 3 different stages is correlated with Fig. 5b. These stages were: at the beginning, with loaders displacement equal to 0 (A), at an intermediate step (B), after approximately 7 mm movement, and near the maximum load, with 13 mm displacement (C).

When the amount of fiber increases, the load reaches higher values. However, the mass fraction variation was not enough to avoid overlapping in the deviations, when comparing plates

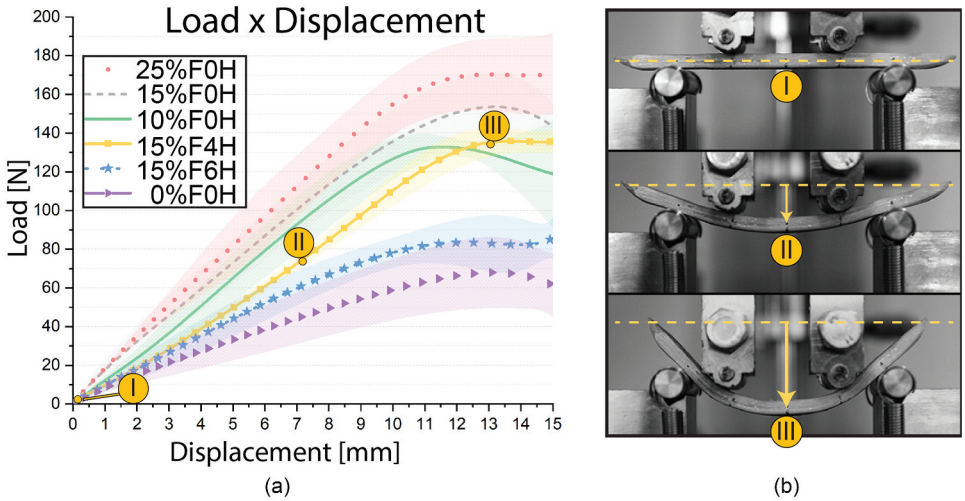

Figure 5. (a) Load versus displacement curves for all the materials analyzed; (b) three test displacement positions for a 15% F4H sample: I) original position, when the test started II) at 7.5mm displacement, III) near the end of the test, when maximum load was reached.

Table 2. Bending stiffness (S), bending structural stiffness (Ele), bending moment (R) and flexural strength for composite implants.

	0%F0 H	10%F0 H	15%F0 H	25%F0 H	15%F4 H	15%F6 H
S [N/mm]	6.00 ± 1.77	13.45 ± 2.290	13.94 ± 1.590	15.77 ± 2.950	10.28 ± 0.230	9.10 ± 1.49
Ele [Nm^2]	0.023 ± 0.007	0.052 ± 0.009	0.054 ± 0.006	0.061 ± 0.012	0.040 ± 0.001	0.035 ± 0.006
M [Nm]	0.582 ± 0.144	1.207 ± 0.065	1.328 ± 0.196	1.504 ± 0.136	1.221 ± 0.052	0.744 ± 0.057
σ_{max} [MPa]	16.56 ± 4.10	34.33 ± 1.84	37.76 ± 5.57	42.79 ± 3.87	34.71 ± 1.47	21.15 ± 1.61

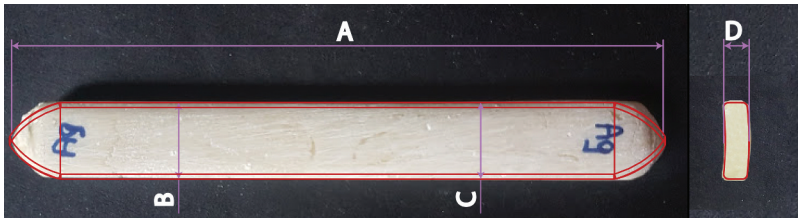

Figure 6. Comparison between the CAD model and the final casted plates. the measure points are marked as A, B, C and D.

Table 3. Dimensional comparison: CAD model versus casted plates.

	A	B	C	D
CAD Model [mm]	116.00	13.50	13.50	4.20
Casted Plates [mm]	114.00 ± 1.60	13.72 ± 0.34	13.70 ± 0.30	4.38 ± 0.20
Average Error	1.75%	1.60%	1.46%	4.11%
Max. Error	3.20%	3.85%	3.57%	7.08%

with 25% and 15% of glass fibers. In addition, differences between 10 and 15 wt% in reinforcements were very pronounced until 11 mm displacement.

After reaching a displacement of approximately 11 mm, there were no major changes in loading. Even though, the curves for 15%F0 H and 10%F0 H samples showed a final downward trend, demonstrating the beginning of their rupture. However, in none of the plates, the total fracture occurred during the test and, so it finished when the displacement reached 15 mm, because some load applicators surfaces, in addition to the rollers, were on the verge of contacting with the samples.

Since the reinforcement is stiffer and more resistant than the matrix, proportionally with the fiber amount increase, there is an increase in the stiffness and strength limit. Also, because of the different transversal areas, hole insertions decreased these values. All the results obtained are presented in Table 2.

In order to compare the geometric structure, all the samples were manually measured using a 0.02 mm precision vernier caliper at the points shown in Fig. 6. The caliper used was a Mitutoyo 0–150 mm, 0,02 mm metric, and all the measurement was done inside the metrology laboratory with controlled environment. Calibrations for this caliper is carried out by the laboratory technician using gauge blocks as reference.

Measurement results and CAD values are shown in Table 3. The average width and thickness of the casted material were bigger than the original CAD model due to a small expansion of the mold during the resin injection. These values were 1.6%, 1.46% and 4.11% higher than those of the CAD reference for measured points B, C and D, respectively.

The length of the plates was, in general, smaller than the models. It occurred because in some samples the ends were not completely filled due to the high viscosity of the resin, preventing it from flowing correctly to these points. However, since the higher reduction caused by it was of 1.8 mm on each side of plates that had 116 mm total, these deviations did not generate major changes in the geometry of the plates.

The SEM results, presented in Fig. 7, show how were the internal structure and the interface between fiber and matrix, highlighting (a) pores, in darker gray in; (b) fibers, in blue, inside a darker-represented matrix; and (c) a region rich in fibers (white) near a pure matrix part. Special attention was

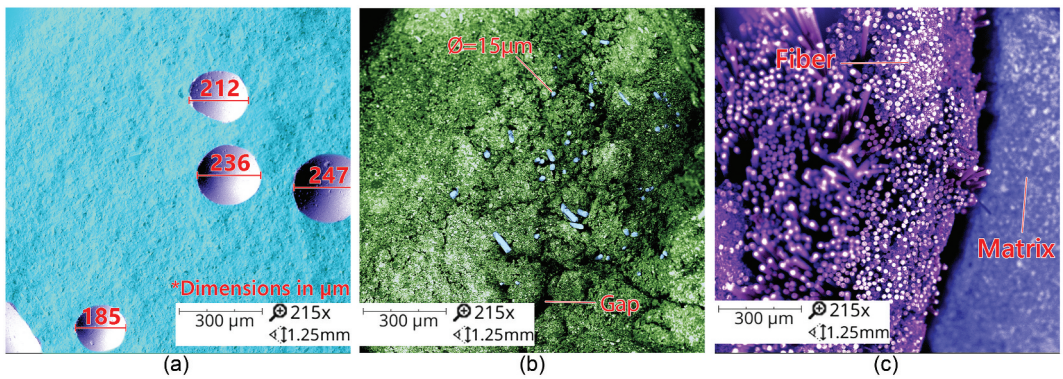

Figure 7. Scanning electron micrograph of the fracture surface: (a) Pure PU sample with pores highlighted; (b) 10% PU glass fibers reinforced composites: fiber diameter and gaps are showed; (c) 15% PU glass fibers reinforced, fiber rich regions are highlighted.

paid to the measurements of the pores and fibers. Also, the distribution and the gaps between the fibers and the matrix were seen with more accuracy.

4. Discussion

4.1. Bending test results discussion

Currently, there are few studies comparing different plate systems and materials, most of them analyze the stress on implants fixed on bones.[13,44] In addition, there is not a single standard for the presentation of the results. For instance, regarding stiffness, some authors establish comparisons between force and displacement in the linear region of the material (N/mm)[45]; others use relations with force and bending angle (N/degree)[33] still, some presents results for bending structural stiffness (Nm^2).[13] So, a challenge to overtake was to establish comparisons with different authors, because of the complex, diverse, and heterogeneous literature about bone plates.[46]

Studies showed satisfactory clinical results when using composite implants with 6 holes for fixation of human tibia fractures, allowing quick bone healing.[47] Fujihara (2003) studied A PEEK (Polyether ether ketone) matrix combined with almost 50% fiber fraction of braided carbon and reached a maximum bending moment between 7.07 and 8.14 Nm, about 40% of the value achieved for stainless-steel plates (18.5 Nm).[31] In this work, the highest value obtained was 1.50 Nm, for 25%GF plates. This value is almost 5 times smaller than that one presented by the braided carbon/PEEK but it can be considered acceptable as the fiber ratio was also smaller.

The bending structural stiffness for reinforced implants variated between 0.035 and 0.061 Nm^2, values compatibles with thin 1.2 mm 7 holes DCP plates that present 0.046 Nm^2. These thin plates are mainly used in small animals, but were also pointed as an alternative to cases where less rigid fixation is needed.[48] For real tibia applications, these values are still low since previous studies reached values between 1.77 and 8.81 Nm^2 for 6 holes carbon epoxy tibial plates.[49,50]

4.2. Advantages of the manufacturing process used

Firstly, references proved that additional holes increase the risk of implant breakage.[51] This occurs due to small freedom when choosing the screws positioning. Nonetheless, reducing the number of holes from 6 to 4, the maximum bending moment increases by 64%, from 0.744 to 1.221 Nm. This demonstrates that a process able to use composite plate manufacturing without holes is an advantageous alternative, because they are easier to drill during the surgery when compared to metallic implants.[52] Hence, it will improve surgeon freedom when choosing a safe position for the screws, in which guarantee the best support for the efforts present in each type of fracture.

In addition, the adapted casting process was cost-efficient, easy to use and highly customizable when compared with another technique that uses polymer or composite fabrication. Traditional gravity casting usually consist only in pouring the resin in a mold, without any injection system or outlet air channel.[53] Consequently, degassing process usually is done only before the casting. Others polymer/composite manufacturing processes, usually need specific machinery and equipment, making these very expensive or only available in large-scale industrial processes.[28,54]

Still, the use of 3D printing and silicone molds ensured great dimensional accuracy, showing only minor deviations when compared with the projected geometry. Thus, because these materials are inexpensive and cure quickly, a wide range of prostheses can be manufactured, according to the requirements of each application, being this one of the factors that make the process flexible.

4.3. SEM analyses

The electron microscopy images showed the existence of pores with diameters up to 247 micrometers and regions of separation between the fiber and matrix. Because the presence of these regions and pores were not uniform all over the tested samples; the deviations of the results presented are justified. Furthermore, the presence of pores also justifies the maximum stresses in samples with 10 and 15% of fibers to have achieved

Table 4. Mechanical properties of bones, fibers, polymers and metals.

	Young's Modulus [GPa]	Poisson Ratio	Tensile Strength [MPa]	Elongation at break [%]	Reference
Cortical Bone[1]	8.5–19.1	0.141	107-146		[56,57]
Trabecular Bone[1]	1.1	0.3	3-20		[56,58]
PU SikaForce 7710L100[2]	0.33[a]	-	13	8	[59]
E-glass fibres[2]	72.3		521	4.8	[60]
Ti-alloy[3]	116	-	965		[11,57]
Co-Cr alloy[3]	210	-	1085		[11,57]
Stainless Steel 316[3]	190	0.3	586	55	[11,57,61,62]
Glass/Polypropylene[4]	5.3	0.098	-	5	[58]
PEEK[4]	8.3	-	139	3	[57,63]
Bioglass[4]	35	-	42		[57]
HDPE[4]	0.88	-	35	-	[11,63]
PU Kehl[4]	1.715	0.440	40	-	[64,65]

[a]Obtained experimentally at preliminary tests according to ASTM D638.
[1]Bone tissues average values based on the references presented.
[2]Materials used in this work; data based on manufacturers datasheet and ASM materials reference book.
[3]Metallic materials for biomedical applications.
[4]Polymers and composites studied or proposed for biomedical applications.

almost similar results. Cracks started in void regions, reducing, consequently, the resistance of the implants, which caused more impact in the results than small increases in the fibers' ratio.

Regions rich in fibers showed low resin impregnation due to the high viscosity of the matrix, as showed in Fig. 5.

Thus, improvements in degassing and, mainly, a surface treatment of the fibers are recommended.[55]

4.4. Material advances for bone plates

The described process also can be used with a wide range of biomaterials, allowing changes in the matrix type and fiber. Fraction of these can be increased to reach properties near the one showed by bones, promoting great advances for bone plates materials.

Table 4 shows the comparison between some of the materials already used in implants, other alternatives, and the bone properties. The Elastic Modulus of metals are 13.6–24.7 times higher than those of hard tissues, which can generate stress-shielding phenomenon. Also, some typical biopolymers did not show strength compatible with these bones.

However, fiber reinforced polymers can be selected to tailor properties that assure stiffness and strength enough to avoid shielding and breakage. By changing the properties of the phases, following the rule of mixtures, it's possible, for instance, to use a polyurethane resin with tensile strength and Young's Modulus higher than the one used in this work, resulting in an enhancement of the composite properties.[66]

Besides that, it is possible to make inner part modifications to allow different amounts of fiber to be inserted along the length of the plate. This improvement makes possible the creation of stiffness-graded implants, in which, are able to reduce the movement near the fracture cortex without shielding distal regions.[50]

The materials and geometries necessary for these changes are already being developed and are the second stage of this research.

5. Conclusions

Comparing the bending structural stiffness of reinforced and non-reinforced plates; a fiber amount increase between 10 and 25 wt% results in a 126% −165% raise in this property. Although the strength and stiffness obtained were low, if other changes are made, such as a larger fiber increase, it is possible to achieve responses closer to those needed in the bone.

The adopted procedures also allowed the fabrication of plates without holes, allowing greater freedom to the surgeon who can select the best screws positions, according to each clinical case, and perform the drilling during the surgical process.

About the process, in comparison with other methods used for the composites manufacturing or polymers, lower cost was observed, since metallic molds or advanced machines were not necessary. It was also highly customizable due to the use of rapid prototyping and elastomeric molds, and it allowed the development of complex geometries, proving to be an effective alternative for the manufacture of non-flat devices. Finally, it proved to be efficient for thermosets, supporting simultaneous injection and air bubbles removal.

Futures studies are recommended including (1) changes in the fibers mass fraction and matrix type, aiming to achieve higher values of bending stiffness and maximum bending moment; and (2) changes in the geometry of the core to allow variation in the amount of fiber along the length of the plate, to produce implants with variable stiffness; and (3) cytotoxicity and other biocompatibility "*invitro*" tests to avoid any unwanted reaction with the biological tissues.

Disclosure statement

No potential conflict of interest was reported by the author(s).

Funding

Foundation for Science and Technology (FCT, Portugal) and FEDER under Programme PT2020 for financial support to CIMO [UIDB/00690/2020] and national funding by FCT, PI, through institutional scientific employment program-contracts. Sika, for the material donations.

References

[1] Black, C. R. M.; Goriainov, V.; Gibbs, D.; Kanczler, J.; Tare, R. S.; Oreffo, R. O. C. Bone Tissue Engineering. *Curr. Mol. Biol. Rep.* 2015, *1*(3), 132–140. DOI: 10.1007/s40610-015-0022-2.

[2] Hernigou, P.; Pariat, J. History of Internal Fixation (Part 1): Early Developments with Wires and Plates Before World War II. *Int. Orthop*. 2017, *41*(6), 1273–1283. DOI: 10.1007/s00264-016-3347-4.

[3] Hernigou, P., and Pariat, J.*Int. Orthop*. 2017 History of Internal Fixation (Part 1): Early Developments with Wires and Plates before World War II, *41* 1489–1500. DOI: 10.1007/s00264-016-3347-4.

[4] Jaul, E.; Barron, J. Age-Related Diseases and Clinical and Public Health Implications for the 85 Years Old and Over Population. *Front Public Health*. 2017, *5*. DOI: 10.3389/fpubh.2017.00335.

[5] de Moura, A. P.; da Silva, E. H.; dos Santos, V. S.; Galera, M. F.; Sales, F. C.; Elizario, S.; de Moura, M. R.; Rigo, V. A.; da Costa, R. R. Structural and Mechanical Characterization of Polyurethane-CaCo3 Composites Synthesized at High Calcium Carbonate Loading: An Experimental and Theoretical Study. *J. Compos. Mater*. 2021, *55*(21), 2857–2866. DOI: https://doi.org/10.1177/0021998321996414 .

[6] Thorén, H.; Snäll, J.; Salo, J.; Suominen-Taipale, L.; Kormi, E.; Lindqvist, C.; Törnwall, J. Occurrence and Types of Associated Injuries in Patients with Fractures of the Facial Bones. *J. Oral Maxillofac. Surg*. 2010, *68*(4), 805–810. DOI: 10.1016/j.joms.2009.09.057.

[7] . Cleveland Clinic. Bone Fractures. *Dis. Conditions*. 2020.

[8] van Oostwaard, M. Osteoporosis and the Nature of Fragility Fracture: An Overview. *Fragility Fract. Nurs*. 2018. DOI: https://doi.org/10.1007/978-3-319-76681-2 .

[9] López-Gómez, S. A.; Villalobos-Rodelo, J. J.; Ávila-Burgos, L.; Casanova-Rosado, J. F.; Vallejos-Sánchez, A. A.; Lucas-Rincón, S. E.; Patiño-Marín, N.; Medina-Solís, C. E. Relationship Between Premature Loss of Primary Teeth with Oral Hygiene, Consumption of Soft Drinks, Dental Care and Previous Caries Experience. *Sci. Rep*. 2016, *6*(1), 21147. DOI: 10.1038/srep21147.

[10] Zuo, K. J.; Olson, J. L. The Evolution of Functional Hand Replacement: From Iron Prostheses to Hand Transplantation. *Plast. Surg*. 2014, *22*(1), 44–51. DOI: 10.1177/229255031402200111.

[11] Li, J.; Qin, L.; Yang, K.; Ma, Z.; Wang, Y.; Cheng, L.; Zhao, D. Materials Evolution of Bone Plates for Internal Fixation of Bone Fractures: A Review. *J. Mater. Sci. Technol.* 2020, *36*, 190–208. DOI: 10.1016/J.JMST.2019.07.024.

[12] Magetsari, R.; van der Houwen, E. B.; Bakker, M. T. J.; van der Mei, H. C.; Verkerke, G. J.; Rakhorst, G.; Hilmy, C. R.; van Horn, J. R.; Busscher, H. J. Biomechanical and Surface Physico-Chemical Analyses of Used Osteosynthesis Plates and Screws—potential for Reuse in Developing Countries? *J. Biomed. Mater. Res. Part B Appl. Biomater.* 2006, *79B*(2), 236–244. DOI: 10.1002/jbm.b.30534.

[13] Mariolani, J. R. L.; Belangero, W. D. Comparing the in vitro Stiffness of Straight-DCP, Wave-DCP, and LCP Bone Plates for Femoral Osteosynthesis. *ISRN Orthop.* 2013, *2013*, 1–6. DOI: https://doi.org/10.1155/2013/308753 .

[14] Mehboob, H.; Chang, S.-H. Application of Composites to Orthopedic Prostheses for Effective Bone Healing: A Review. *Compos. Struct.* 2014, *118*, 328–341. DOI: 10.1016/J.COMPSTRUCT.2014.07.052.

[15] Hak, D. J.; Banegas, R.; Ipaktchi, K.; Mauffrey, C. Evolution of Plate Design and Material Composition. *Injury.* 2018, *49*, S8–S11. DOI: 10.1016/S0020-1383(18)30295-X.

[16] da Costa, R. R. C.; de Almeida, F. R. B.; da Silva, A. A. X.; Domiciano, S. M.; Vieira, A. F. C. Design of a Polymeric Composite Material Femoral Stem for Hip Joint Implant. *Polímeros.* 2019, *29*(4). DOI: 10.1590/0104-1428.02119.

[17] Shetty, P.; Yadav, P.; Tahir, M.; Saini, V. Implant Design and Stress Distribution. *Int. J. Oral Implantol. Clin. Res.* 2016, *7*(2), 34–39. DOI: 10.5005/jp-journals-10012-1151.

[18] De Santis, R.; Guarino, V.; Ambrosio, L. Composite Biomaterials for Bone Repair. *Bone Repair Biomater.* 2019, 273–299. DOI: 10.1016/B978-0-08-102451-5.00010-X.

[19] Sathishkumar, T.; Satheeshkumar, S.; Naveen, J. Glass Fiber-Reinforced Polymer Composites – a Review. *J. Reinf. Plast. Compos.* 2014, *33*(13), 1258–1275. DOI: 10.1177/0731684414530790.

[20] Beckett, L. E.; Lewis, J. T.; Tonge, T. K.; Korley, L. T. J. Enhancement of the Mechanical Properties of Hydrogels with Continuous Fibrous Reinforcement. *ACS Biomater. Sci. Eng.* 2020, *6*(10), 5453–5473. DOI: https://doi.org/10.1021/acsbiomaterials.0c00911 .

[21] Lazar, M.-A.; Rotaru, H.; Bâldea, I.; Boşca, A. B.; Berce, C. P.; Prejmerean, C.; Prodan, D.; Câmpian, R. S. Evaluation of the Biocompatibility of New Fiber-Reinforced Composite Materials for Craniofacial Bone Reconstruction. *J. Craniofac. Surg.* 2016, *27*(7), 1694–1699. DOI: https://doi.org/10.1097/SCS.0000000000002925 .

[22] Reis, J. M. L.; Chaves, F. L.; da Costa Mattos, H. S. Tensile Behaviour of Glass Fibre Reinforced Polyurethane at Different Strain Rates. *Mater. Des.* 2013, *49*, 192–196. DOI: 10.1016/j.matdes.2013.01.065.

[23] Boretos, J. W.; Pierce, W. S. Segmented Polyurethane: A New Elastomer for Biomedical Applications. *Science.* 1967, *158*(3807), 1481–1482. DOI: 10.1126/science.158.3807.1481.

[24] Da Costa, R. R. C.; De Medeiros, R.; Ribeiro, M. L.; Tita, V. Experimental and Numerical Analysis of Single Lap Bonded Joints: Epoxy and Castor Oil PU-Glass Fibre Composites. *J. Adhes.* 2017, *93*, 77–94. DOI: 10.1080/00218464.2016.1172212.

[25] Szczepańczyk, P.; Szlachta, M.; Złocista-Szewczyk, N.; Chłopek, J.; Pielichowska, K. Recent Developments in Polyurethane-Based Materials for Bone Tissue Engineering. *Polymers (Basel).* 2021, *13*(6), 946. DOI: 10.3390/polym13060946.

[26] Tanzi, M. C.; Farè, S.; Petrini, P.; Tanini, A.; Piscitelli, E.; Zecchi-Orlandini, S.; Brandi, M. L. Cytocompatibility of Polyurethane Foams as Biointegrable Matrices for the Preparation of Scaffolds for Bone Reconstruction. *J. Appl. Biomater. Biomech.* 2003, *1*(1), 58–66. DOI: 10.1177/228080000300100107.

[27] Huang, Z. Stiffness and Strength Design of Composite Bone Plates. *Compos. Sci. Technol.* 2005, *65*(1), 73–85. DOI: 10.1016/j.compscitech.2004.06.006.

[28] Chohan, J. S.; Boparai, K. S.; Singh, R.; Hashmi, M. S. Manufacturing Techniques and Applications of Polymer Matrix Composites: A Brief Review. *Adv. Mater. Process. Technol.* 2020, 1–11. DOI: 10.1080/2374068X.2020.1835012.

[29] Harper, C. A., and Petrie, E. M. Plastic Materials and Process. In *Plastics Materials and Processes: A Concise Enciclopedia* (Hoboken, New Jersey: John Wiley & Sons, Inc.,), 2003. DOI: 10.1002/0471459216.fmatter.

[30] Asim, M.; Jawaid, M.; Saba, N.; Ramengmawii, Nasir, M.; Sultan, M. T. H. Processing of Hybrid Polymer Composites—a Review. *Hybrid Polym. Compos. Mater.* 2017. DOI: 10.1016/B978-0-08-100789-1.00001-0.

[31] Fujihara, K.; Huang, Z.-M.; Ramakrishna, S.; Satknanantham, K.; Hamada, H. Performance Study of Braided Carbon/peek Composite Compression Bone Plates. *Biomaterials.* 2003, *24*(15), 2661–2667. DOI: 10.1016/S0142-9612(03)00065-6.

[32] Kabiri, A.; Liaghat, G.; Alavi, F.; Saidpour, H.; Hedayati, S. K.; Ansari, M.; Chizari, M. Glass Fiber/polypropylene Composites with Potential of Bone Fracture Fixation Plates: Manufacturing Process and Mechanical Characterization. *J. Compos. Mater.* 2020, *54*(30), 4903–4919. DOI: https://doi.org/10.1177/0021998320940367 .

[33] Park, S.-W.; Yoo, S.-H.; An, S.-T.; Chang, S.-H. Material Characterization of Glass/polypropylene Composite Bone Plates According to the Forming Condition and Performance Evaluation Under a Simulated Human Body Environment. *Compos. Part B Eng.* 2012, *43*(3), 1101–1108. DOI: https://doi.org/10.1016/j.compositesb.2011.09.008 .

[34] Al-Shammari, B.; Al-Fariss, T.; Al-Sewailm, F.; Elleithy, R. The Effect of Polymer Concentration and Temperature on the Rheological Behavior of Metallocene Linear Low Density Polyethylene (MLLDPE) Solutions. *J. King Saud Univ. - Eng. Sci.* 2011, *23*(1). DOI: 10.1016/j.jksues.2010.07.001.

[35] Biswal, T.; BadJena, S. K.; Pradhan, D. Synthesis of Polymer Composite Materials and Their Biomedical Applications. *Mater. Today Proc.* 2020, *30*, 305–315. DOI: https://doi.org/10.1016/J.MATPR.2020.01.567 .

[36] Arumugam, S.; Kandasamy, J.; Md Shah, A. U.; Hameed Sultan, M. T.; Safri, S. N. A.; Abdul Majid, M. S.; Basri, A. A.; Mustapha, F. Investigations on the Mechanical Properties of Glass Fiber/sisal Fiber/chitosan Reinforced Hybrid Polymer Sandwich Composite Scaffolds for Bone Fracture Fixation Applications. *Polymers (Basel).* 2020, *12*(7), 1501. DOI: 10.3390/polym12071501.

[37] Frigg, R. Development of the Locking Compression Plate. *Injury.* 2003, *34*, 6–10. DOI: 10.1016/j.injury.2003.09.020.

[38] Thian, S. C. H.; Tang, Y.; Tan, W. K.; Fuh, J. Y. H.; Wong, Y. S.; Loh, H. T.; Lu, L. The Manufacture of Micromould and Microparts by Vacuum Casting. *Int. J. Adv. Manuf. Technol.* 2008, *38*(9–10), 944–948. DOI: 10.1007/s00170-007-1151-4.

[39] Tong, G. O., and Bavornratanavech, S. *AO Manual of Fracture Management: Minimally Invasive Plate Osteosynthesis (MIPO)*, 1st ed.; Platz, D., Ed.; Davos, Switzerland: AO Publishing: Clavadelerstrasse, 2007.

[40] Bonyár, A.; Sántha, H.; Varga, M.; Ring, B.; Vitéz, A.; Harsányi, G. Characterization of Rapid PDMS Casting Technique Utilizing Molding Forms Fabricated by 3D Rapid Prototyping Technology (RPT). *Int. J. Mater. Form.* 2014, *7*(2), 189–196. DOI: 10.1007/s12289-012-1119-2.

[41] International Organization for Standardization. ISO 9585:Implants for Surgery — Determination of Bending Strength and Stiffness of Bone Plates. 1990. https://www.iso.org/standard/17351.html

[42] Berube, K. A.; Lopez-Anido, R. A.; Goupee, A. J. Determining the Flexural and Shear Moduli of Fiber-Reinforced Polymer Composites Using Three-Dimensional Digital Image Correlation. *Exp. Tech.* 2015, *40*(4), 1263–1273. DOI: https://doi.org/10.1111/ext.12178 .

[43] Hibbeler, R. C., and Sekar, K. S. V. *Mechanics of Materials*; London: Pearson Education, 2013.

[44] Caiti, G.; Dobbe, J. G. G.; Bervoets, E.; Beerens, M.; Strackee, S. D.; Strijkers, G. J.; Streekstra, G. J. Biomechanical Considerations in the Design of Patient-Specific Fixation Plates for the Distal Radius. *Med. Biol. Eng. Comput*. 2019, *57*(5), 1099–1107. DOI: 10.1007/s11517-018-1945-6.

[45] Chakladar, N. D.; Harper, L. T.; Parsons, A. J. Optimisation of Composite Bone Plates for Ulnar Transverse Fractures. *J. Mech. Behav. Biomed. Mater*. 2016, *57*, 334–346. DOI: 10.1016/J.JMBBM.2016.01.029.

[46] Schorler, H.; Wendlandt, R.; Jürgens, C.; Schulz, A.-P.; Kaddick, C.; Capanni, F. Bone Plate-Screw Constructs for Osteosynthesis – Recommendations for Standardized Mechanical Torsion and Bending Tests. *Biomed. Eng./Biomed. Tech*. 2018, *63*(6). DOI: 10.1515/bmt-2017-0126.

[47] Tayton, K.; Johnson-Nurse, C.; McKibbin, B.; Bradley, J.; Hastings, G. The Use of Semi-Rigid Carbon-Fibre-Reinforced Plastic Plates for Fixation of Human Fractures. Results of Preliminary Trials. *J. Bone Joint Surg. Br*. 1982, *64*-B(1), 105–111. DOI: 10.1302/0301-620X.64B1.7040407.

[48] Strom, A. M.; Garcia, T. C.; Jandrey, K.; Huber, M. L.; Stover, S. M. In vitro Mechanical Comparison of 2.0 and 2.4 Limited-Contact Dynamic Compression Plates and 2.0 Dynamic Compression Plates of Different Thicknesses. *Vet. Surg*. 2010, *39*(7), 824–828. DOI: https://doi.org/10.1111/j.1532-950X.2010.00736.x .

[49] Kim, S.-H.; Chang, S.-H.; Son, D.-S. Finite Element Analysis of the Effect of Bending Stiffness and Contact Condition of Composite Bone Plates with Simple Rectangular Cross-Section on the Bio-Mechanical Behaviour of Fractured Long Bones. *Compos. Part B Eng*. 2011, *42*(6), 1731–1738. DOI: https://doi.org/10.1016/j.compositesb.2011.03.001 .

[50] Ramakrishna, K.; Sridhar, I.; Sivashanker, S.; Khong, K. S.; Ghista, D. N. Design of Fracture Fixation Plate for Necessary and Sufficient Bone Stress Shielding. *JSME Int. J*. 2004, *47*, 1086–1094. DOI: https://doi.org/10.1299/jsmec.47.1086 .

[51] Lv, H.; Chang, W.; Yuwen, P.; Yang, N.; Yan, X.; Zhang, Y. Are There Too Many Screw Holes in Plates for Fracture Fixation? *BMC Surg*. 2017, *17*(1), 46. DOI: 10.1186/s12893-017-0244-8.

[52] Fernández-Pérez, J.; Cantero, J.; Díaz-Álvarez, J.; Miguélez, M. Hybrid Composite-Metal Stack Drilling with Different Minimum Quantity Lubrication Levels. *Mater. (Basel)*. 2019, *12*(3), 448. DOI: 10.3390/ma12030448.

[53] Kuo, C. C.; Wang, Y. J.; Shi, Z. S. Development of a High Precision Silicone Rubber Mold for Cylinder Block. *Appl. Mech. Mater*. 2013, *459*, 342–348. DOI: 10.4028/AMM.459.342.

[54] Bhatt, A. T.; Gohil, P. P.; Chaudhary, V. Primary Manufacturing Processes for Fiber Reinforced Composites: History, Development & Future Research Trends. *IOP Conf. Ser Mater. Sci. Eng*. 2018, *330*, 012107. DOI: https://doi.org/10.1088/1757-899X/330/1/012107 .

[55] Cadore-Rodrigues, A. C.; Guilardi, L. F.; Wandscher, V. F.; Pereira, G. K. R.; Valandro, L. F.; Rippe, M. P. Surface Treatments of a Glass-Fiber Reinforced Composite: Effect on the Adhesion to a Composite Resin. *J. Prosthodont. Res*. 2020, *64*(3), 301–306. DOI: 10.1016/j.jpor.2019.09.001.

[56] Court-Brown, C. M.; Heckman, J. D.; McQueen, M. M.; Ricci, W. M.; Tornetta, P., and McKee, M. D. Rockwood and Green's Fractures in Adults;*Rockwood and Green's Fractures in Adults*; Philadelphia: Wolters Kluwer Health, 2015.

[57] Ramakrishna, S.; Mayer, J.; Wintermantel, E.; Leong, K. W. Biomedical Applications of Polymer-Composite Materials: A Review. *Compos. Sci. Technol*. 2001, *61*(9), 1189–1224. DOI: https://doi.org/10.1016/S0266-3538(00)00241-4 .

[58] Mehboob, A.; Chang, S.-H. Effect of Composite Bone Plates on Callus Generation and Healing of Fractured Tibia with Different Screw Configurations. *Compos. Sci. Technol*. 2018, *167*, 96–105. DOI: https://doi.org/10.1016/j.compscitech.2018.07.039 .

[59] Sika. Product Datasheet: SikaForce®-7710 L100, *SikaForce*. 2012 https://prt.sika.com/dms/getdocument.get/596171ed-ac85-3274-b893-1ee164a36355/SikaForce_7710_L_100-pt-02.2012.pdf

[60] Bauccio, M. *ASM Engineered Materials Reference Book*, 2nd.; London: ASM InternationalMaterials Park, OH: 1994;

[61] Baharnezhad, S.; Farhangi, H.; Allahyari, A. A. Influence of Geometry and Design Parameters on Flexural Behavior of Dynamic Compression Plates (Dcp): Experiment and Finite Element Analysis. *J. Mech. Med. Biol*. 2013, *13*(3), 1350032. DOI: https://doi.org/10.1142/S0219519413500322 .

[62] Fouda, N.; Mostafa, R.; Saker, A. Numerical Study of Stress Shielding Reduction at Fractured Bone Using Metallic and Composite Bone-Plate Models. *Ain Shams Eng. J*. 2019, *10*(3), 481–488. DOI: https://doi.org/10.1016/J.ASEJ.2018.12.005 .

[63] Banoriya, D.; Purohit, R.; Dwivedi, R. K. Study of Particle Dispersion on One Bed Hospital Using Computational Fluid Dynamics. *Mater. Today Proc*. 2017, *4*(2), 10074–10079. DOI: https://doi.org/10.1016/j.matpr.2017.02.244 .

[64] . Kehl. Product Datasheet: Aglomerante Kehl Ag101. KehlIndustry. 2021, http://www.kehl.ind.br/catalogos/KEHL_-_Aglomerante_1.pdf

[65] da Silva, E. H. P.; Almendro, E. B.; da Silva, A. A. X.; Waldow, G.; Sales, F. C. P.; de Moura, A. P.; da Costa, R. R. C. Manufacture and Mechanical Behavior of Green Polymeric Composite Reinforced with Hydrated Cotton Fiber. *J. Exp. Tech. Instrum*. 2019, *2*, 1. DOI: 10.30609/JETI.2019-7576.

[66] Clayton, C. R. *Materials Science and Engineering: An Introduction*, Wiley: Chichester, West Sussex, 1987; Vol. 94. DOI: 10.1016/0025-5416(87)90343-0.